Functional Microswitches of Mammalian G Protein-Coupled Bitter-Taste Receptors

Jérémie Topin[‡,1,*], Cédric Bouysset[‡,1], Yiseul Kim[2], MeeRa Rhyu[2], Sébastien Fiorucci[1,*], Jérôme Golebiowski[1,3]

[‡] Co-first authors
[1] Dr. J. Topin, C. Bouysset, Dr. S. Fiorucci, Prof. J. Golebiowski
Institut de Chimie de Nice UMR7272
Université Côte d'Azur, CNRS, France
E-mail: jeremie.topin@univ-cotedazur.fr; sebastien.fiorucci@univ-cotedazur.fr
[2] Prof. M. Rhyu, Y. Kim
Korea Food Research Institute
245 Iseo-myeon, Wanju-gun, Jeollabuk-do 55365, South Korea
[3] Prof. J. Golebiowski
Dept. of Brain & Cognitive Sciences, DGIST, 333, Techno JungAng
Daero, HyeongPoong Myeon, Daegu, 711-873, Rep. of Korea

Abstract: Bitter taste receptors (TAS2Rs) are a poorly understood subgroup of G protein-coupled receptors (GPCR). No experimental structure of these receptors is available and key-residues controlling their function remain mostly unknown. Here, we have identified the functional microswitches that encode agonist sensing and downstream signaling mechanisms within TAS2Rs sequences. We thoroughly re-aligned the amino-acid sequences of the 25 human TAS2Rs considering residue conservations and all the experimental data from the literature as constraints. As a test case, an accurate homology model of TAS2R16 was constructed and examined by site-directed mutagenesis and *in vitro* functional assays. Conserved motifs acting as microswitches during agonist-sensing and receptor activation were pinpointed by comparison with the current knowledge on class A GPCRs. Unravelling these sequence – function relationships is of utmost importance to streamline how TAS2Rs functions are encrypted in their sequence.

Bitterness is one of the basic taste modalities detected by the gustatory system. It is generally considered as a warning against the intake of noxious compounds[1] and, as such, is often associated with disgust and avoidance of foods.[2]

At the molecular level, this perception is initiated by the activation of bitter taste receptors. In humans, 25 genes functionally express these so-called taste receptors type 2 (TAS2Rs), endowing us with the capacity to detect a wide array of bitter chemicals.[3] Interestingly, TAS2Rs are also ectopically expressed in non-chemosensory tissues, emerging as important pharmacological targets.[4]

TAS2Rs are G protein-coupled receptors (GPCRs) and are classified as distantly related to class A GPCRs.[5] Structurally, GPCRs are made up of seven transmembrane helices, named TM1 to TM7, which form a bundle across the cell membrane. How GPCRs achieve specific robust signaling and how these functions are encoded into their sequences are pending fundamental questions.

GPCR activation relies on so-called microswitches, which allosterically connect the ligand binding pocket to the intracellular G protein coupling site to trigger downstream signaling.[6] In class A GPCRs (including olfactory receptors, ORs), these microswitches consist of conserved sequence motifs (Figure 1). The "toggle/transmission switch" CWxP^{TM6} (or FYGx^{TM6} in ORs) sense agonists, whereas the other motifs propagate the signal: the "hydrophobic connector" PIF$^{TM3-5-6}$, the NPxxY^{TM7}, the "ionic lock"DRY^{TM3} and a "hydrophobic barrier" between the last two.[7]

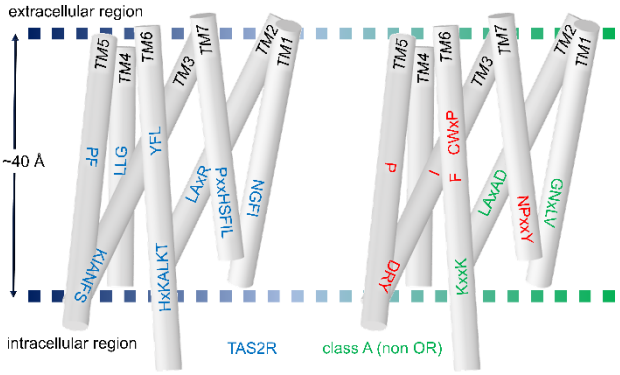

Figure 1. TAS2R (left) and non-olfactory class A GPCR (right) sequence hallmarks labelled on each transmembrane helix. In non-olfactory class A GPCR, functional microswitches are highlighted in red.

No experimental structure is available for any TAS2R to date, yet hallmark motifs have been defined based on sequence conservation: NGFI^{TM1}, LAxSR^{TM2}, KIANFS^{TM3}, LLG^{TM4}, PF^{TM5}, HxKALKT^{TM6}, YFL^{TM6}, and PxxHSFIL^{TM7}.[5] The sequence similarity between TAS2Rs and class A GPCRs is typically in the range 14%-29%[8] and the conserved motifs are hardly comparable (Figure 1, Table S1). Thus, sequence alignment between TAS2Rs and class A GPCRs is non-trivial. Existing alignments differ in TM3, TM4, TM6 or TM7,[8-9] making it difficult to infer TAS2R functional microswitches. This remains a central issue in understanding the complex allosteric TAS2R machinery. The present study aims at identifying the microswitches that control TAS2R functions. Site-directed mutagenesis followed by functional assays *in vitro* on human TAS2R16, used as a case study, further assessed the roles of the predicted microswitches in TAS2Rs.

We previously established the alignment of ORs with non-olfactory class A GPCRs by a large amount of experimental data.[7b, 7d, 11] To overcome the lack of sequences similarity

between TAS2Rs and GPCRs with known structures, we inserted 339 human class II OR sequences in the alignment. Manual curation was performed afterwards by integrating site-directed mutagenesis data from the literature, which covers 120 amino-acids positions, i.e. 35% of the whole TAS2R sequence or 50% of the TM domain (see supporting files). Our alignment highlights the key-residues and consensus motifs in all human TAS2Rs, which correspond to the functional microswitches in ORs and non-olfactory class A GPCRs. They are summarized in Table 1.

Table 1. Key-residues and consensus motifs in TAS2R, OR, and non-olfactory class A GPCR TM helices. Superscripts refer to the Ballesteros–Weinstein numbering scheme.[12]

TM	TAS2R	OR	class A GPCR
1	$N^{1.50}$GFI	$GN^{1.50}$LLI	$GN^{1.50}$xLV
2	LAxS$R^{2.50}$	LSFx$D^{2.50}$	LAxA$D^{2.50}$
3	$L^{3.43}$ $K^{3.50}$IANFS	$L^{3.43}$ MAYD$R^{3.50}$YVAIC	$L^{3.43}$ D$R^{3.50}$Y
4	$L^{4.50}$LG	$W^{4.50}$	$W^{4.50}$
5	$P^{5.50}$F $F^{5.58}$	$P^{5.50}$F $Y^{5.58}$	$P^{5.50}$ $Y^{5.58}$
6	HxK$^{6.32}$ALKT YF$^{6.48}$L	RxK$^{6.32}$AFSTC FY$^{6.48}$G	K$^{6.32}$xxK CW$^{6.48}$LP
7	PxxHS$^{7.50}$FIL	PxxNP$^{7.50}$xIY	SxxNP$^{7.50}$xxY

TM1, 2 and 4 do not contain motifs involved in downstream signaling. In TM1, the NGFI$^{TM1\text{-}TAS2R}$ motif corresponds to GNLLI$^{TM1\text{-}OR}$ in OR and GNxLV$^{TM1\text{-}classA}$ in non-olfactory GPCR templates (see Figure S1). In TM2, $R^{2.50\text{-}TAS2R}$ in the LAxSR$^{TM2\text{-}TAS2R}$ motif aligns with $D^{2.50\text{-}OR/classA}$, which in class A GPCRs constitutes a sodium ion binding site that stabilizes inactive receptor conformations.[13] Position 2.50 in TAS2Rs is positively-charged and is unlikely to be involved in sodium binding. It is rather hypothesized to stabilize the structure of TAS2Rs.[9c] The alignment of TM4 is not straightforward as it lacks the canonical $W^{4.50\text{-}OR/classA}$. The highly conserved leucine $L^{4.50}$ of the LLG$^{TM4\text{-}TAS2R}$ motif was aligned to the most conserved $W^{4.50\text{-}OR/class\ A}$.

TM3, 5, 6, and 7 contain functional microswitches which have been identified in class A GPCR experimental structures.[6] Figure 2 focuses on the alignment between TAS2Rs, ORs, and non-olfactory class A GPCRs for these TM domains.

In TM3, $K^{3.50}$ in the KIANFS$^{TM3\text{-}TAS2R}$ motif matches $R^{3.50}$ of the DRY$^{TM3\text{-}classA}$ and MAYDRYVAIC$^{TM3\text{-}OR}$ motifs. The DRY motif constitutes the 'ionic lock' in ORs and non-olfactory class A GPCRs. This also aligns $L^{3.43}$ which is conserved in all the three families.

In TM5, the conserved $P^{5.50}$ of the PF$^{TM5\text{-}TAS2R}$ motif aligns with the PF$^{TM5\text{-}OR}$ and $P^{TM5\text{-}classA}$ motifs/residue involved in the so-called 'hydrophobic connector' ($P^{5.50}I^{3.40}F^{6.44}$ in class A GPCRs). Another conserved aromatic residue $F^{5.58}$ (found in 52% of TAS2Rs) consistently aligns with the conserved $Y^{5.58}$ known to be important for GPCR activation.[7d, 14]

In TM6, the HxKALKT$^{TM6\text{-}TAS2R}$ motif matches a comparable motif in non-olfactory class A GPCR and the typical OR motif RxKAFST$^{TM6\text{-}OR}$. The 'toggle/transmission switch' (CW$^{6.48}$LP^{classA} and FY$^{6.48}$G^{OR}) aligns with the YF$^{6.48}$L motif in TAS2Rs. The location of this YF$^{6.48}$L motif (at the bottom of the pocket, see Figure S1) is consistent with several site-directed mutagenesis data suggesting their ligand-sensing roles, as is the case for class A GPCRs.[7b, 15]

The extracellular part of TM7 is well documented to belong to the ligand binding pocket in TAS2Rs and other GPCRs.[9b, 9f, 15] This is consistent with the high sequence variability (see Figure S1). The intracellular residues show higher conservation, as they are involved in the signaling of GPCR.[7b, 15] The conserved motifs are however hardly comparable between TAS2Rs and other GPCRs. The comparison with ORs is here highly instructive: the $P^{7.46}$xLNP$^{7.50}$xIY$^{TM7\text{-}OR}$ motif in ORs shares $P^{7.46}$ with TAS2Rs and NP$^{7.50}$xxY with other class A GPCRs. $P^{7.46}$ and $P^{7.50}$ are conserved in 76% and 28% of human TAS2Rs, respectively. The PxxHSFIL$^{TM7\text{-}TAS2R}$ motif is consequently aligned with PxLNPxIY$^{TM7\text{-}OR}$, which itself matches the highly conserved xxxNPxxY$^{TM7\text{-}classA}$ motif.[9b]

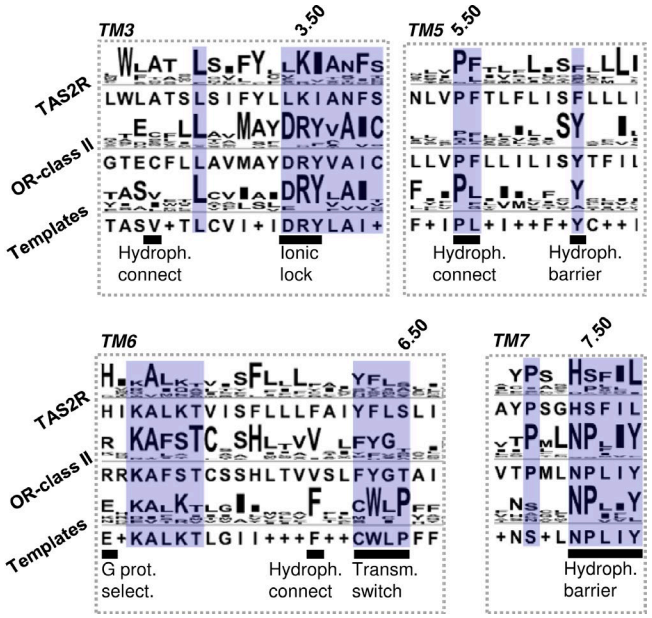

Figure 2. Showlogo of human TAS2R (TAS2R), human class II OR (OR-class II) and non-OR class A GPCR templates sequences. The aligned motifs are highlighted in blue. Functional microswitches identified in experimental structures are underlined (Hydrophobic connector, Ionic lock, Hydrophobic barrier, G protein selection, and Transmission switch). Consensus sequences for TAS2Rs, ORs and templates contain respectively 25 human TAS2Rs, 339 human class II ORs and 6 class A GPCRs (see Figure S1).

Based on this alignment, we tested various protocols and structural templates to build an accurate 3D homology model. The best model was obtained using a multi-template protocol combining the β2-adrenergic receptor[16] and the chemokine receptor CXCR4[17] structures. Projecting the TAS2R sequence conservation onto the 3D model showed that the most conserved residues faced each other in the intracellular part (see Figure S3), while the most variable positions were in the ligand binding pocket.

To assess the functional role of the predicted microswitches, twelve residue positions were subjected to site-directed mutagenesis followed by *in vitro* functional assays with salicin on TAS2R16 (Table S2, Figure 3). The residues mostly belong to

TM3 and TM6 which are well documented in GPCRs to be involved in agonist sensing and activation.[6] Based on our model, we investigated residues in the ligand binding pocket (90$^{3.35}$, 91$^{3.36}$,185$^{5.47}$) and at or around the predicted microswitches (45$^{2.38}$, 97$^{3.41}$, 221$^{6.29}$, 222$^{6.30}$, 236$^{6.44}$ and 239$^{6.47}$). Residues 42^{ICL1}, 43^{ICL1}, and 100$^{3.44}$ were predicted to be far from the microswitches.

As negative controls (Table S2), L42^{ICL1}A/S, M43^{ICL1}A and T100$^{3.44}$A mutations consistently did not affect the response of the receptor to salicin. Mutation of position 43 to serine in ICL1 induced a moderate but significant increase on salicin-induced TAS2R16 response (Figure 3 and Table S3).

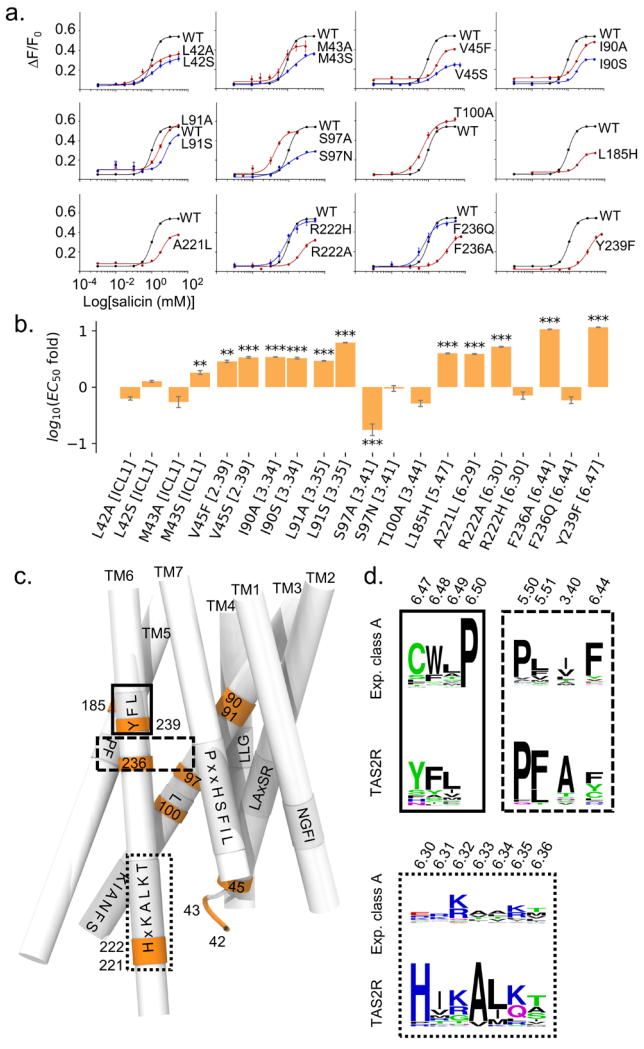

Figure 3. a) *In vitro* functional assays of wild-type TAS2R16 (WT) and single-point mutants stimulated by salicin. b) EC50 fold (compared to WT) expressed as log($EC_{50}^{MUT}/EC_{50}^{WT}$) for the 20 TAS2R16 mutants considered in this study. Positive values indicate a lower response of the receptor to salicin compared to the WT. *** p < 0.001, ** p <0.01, and * p < 0.05 *versus* the WT group (one-way ANOVA followed by Dunnett's test) c) Representative structure of TAS2R16 highlighting the location of the mutated residues. The TM domain is presented as sticks. Position of residues mutated are coloured in orange, and the microswitches revealed by the sequence alignment are boxed. d) Show logo of conserved motifs involved in the activation mechanism of TAS2Rs and class A GPCRs, i.e. the transmission switch (boxed in plain lines), the hydrophobic connector (boxed in dashed lines) and the G-protein coupling region (boxed in dotted line).

TASR216 I90A/S$^{3.35}$, L91A/S$^{3.36}$, L185H$^{5.47}$ mutants showed impaired responses to salicin, consistent with their orientation toward the interior of the receptor bundle and previous reports of their interaction with ligands.[9h, 9l, 18]

The hydrophobic connector microswitch, involved in receptor activation[7a], is conserved as P$^{5.50}$I$^{3.40}$F$^{6.44}$ in class A GPCRs.[6-7, 7c] It is conserved as P$^{5.50}$A$^{3.40}$F$^{6.44}$ in TAS2R (see Figure 3c) and is located at the core of TAS2R16, close to the cradle of the binding pocket. In class A GPCRs, it is associated, together with NPxxY^{TM7}, with a central role in receptor signaling, ligand-independent constitutive activation, and β-arrestin signaling in the β_2AR.[7c] Similar functions are conceivable in TAS2R[19] as suggested by the modulated response to salicin upon our mutations (Figure 3), and those in the literature.[9h, 18] F236$^{6.44}$ (conserved in 60% of TAS2Rs as Y/F) is predicted to be part of the so-called 'hydrophobic connector' microswitch. The F236A$^{6.44}$ TAS2R16 mutant consistently showed a significant weaker response to salicin, while F236Q$^{6.44}$ mutant showed no difference. Next to position 3.40, S97$^{3.41}$ does not belong to the binding pocket (see Figure S3) and points toward the membrane. In agreement with a previous report showing its importance for TAS2R16 trafficking,[9h] S97A$^{3.41}$ mutation affects receptor response (gain of function).

Position 239$^{6.47}$ is conserved as Y (64%) and F (8%) in TAS2Rs. Such a conservation as aromatic is also found in ORs.[7b] The Y239F$^{6.47}$ mutation decreased the salicin potency by a factor 11, confirming its importance in receptor activation. This underlines the relevance of matching the Y$^{6.47}$FLx motif in TAS2Rs with F$^{6.47}$YGx in ORs[7b] and C$^{6.47}$WLP[6] in non-olfactory class A GPCRs. This motif is particularly important as it contributes to the cradle of the binding pocket and senses the presence of agonists.[15] Adjacent to Y239$^{6.47}$, F240$^{6.48}$ is conserved as aromatic in 72% of TAS2Rs. As the toggle-switch residue, it is consistently located at the cradle of the binding cavity in our 3D model. Its nature and function in agonist-sensing is similar in ORs (conserved as F$^{6.48}$)[7b] and non-olfactory GPCR (conserved as W$^{6.48}$)[6]. F240$^{6.48}$ has already been reported to affect TAS2R16 response to agonists by Sakurai et al. who showed that mutation of F240$^{2.48}$ to a Leucine residue in TAS2R16 drastically alters the function of the receptor, while the mutation to aromatic residues (Y and W) leads to moderate EC50 changes.[9a] Note that the response to various agonists was affected in the same manner, highlighting its critical role in initiating the signal, as is the case for numerous class A GPCRs.[6-7]

Our model predicted that V45$^{2.38}$ is involved in a hydrophobic cluster at the intracellular part of TM2 and is conserved as a hydrophobic residue in 72% of TAS2Rs. This hydrophobic patch is in the vicinity of the highly conserved L229$^{7.53}$ of the HSFIL^{TM7} motif and is likely part of the 'hydrophobic barrier' preventing the flooding of the intracellular region. Mutating V45$^{2.38}$ into a hydrophilic residue (S) strongly altered the response to salicin in both our work and the literature[9h], whereas substitution by a bulkier hydrophobic residue (F) was better tolerated.

In TM6, position 221$^{6.29}$ and vicinal residues are documented to control the selectivity for G proteins in class A GPCRs through positive charges.[20] A221$^{6.29}$ and H222$^{6.30}$ are conserved in 60% and 92% of TAS2Rs, respectively (position 222$^{6.30}$ is an arginine for TAS2R16). The A221L$^{6.29}$ and R222A$^{6.30}$ mutants thus induced decreased responses to salicin whereas the R222H$^{6.30}$ mutant showed no statistical difference compared to WT. This

highlights the need of a positive charge at position 6.30 for G protein coupling and selectivity.

This study has unraveled key-residues and consensus functional motifs of TAS2Rs using a combination of bioinformatics, molecular modeling and *in vitro* assays. The consensus sequence motifs match the well-known ones in class A GPCRs. Besides, we provided a thorough sequence alignment of human bitter-taste receptors with olfactory and non-olfactory class A GPCR, integrating residues conservation and experimental data as constraints. Site-directed mutagenesis then allowed us to assess the functional roles of these motifs in the TAS2R16 case study. In addition to residues lining the binding pocket, we identified the "toggle/transmission switch" (the $YF^{6.48}L$ motif in TM6) and the "hydrophobic connector" ($P^{5.50}A^{3.40}F^{6.44}$) for agonist sensing. Other microswitches were identified at the intracellular part of TM6/TM7 that are suggested to be involved in the selectivity for the G protein or in receptor activation. The nature of these microswitches extends to mammalian TAS2Rs (see supporting files). The approach, templates, and 3D model provide solid grounds for rational design of specific TAS2R agonists and antagonists, and for decoding the sequence-structure-function relationships in these receptors.

Acknowledgements

The authors thank Dr. Xiaojing Cong and Jody Pacalon for the fruitful discussions and critical reading of the manuscript. This work was funded by the French Ministry of Higher Education and Research [PhD Fellowship to CB], by the National Research Foundation of Korea (NRF) [grant number NRF2020R1A2C2004661], by GIRACT (Geneva, Switzerland) [9th European PhD in Flavor Research Bursaries for first year students to CB] and the Gen Foundation (Registered UK Charity No. 1071026) [a charitable trust which principally provides grants to students/researchers in natural sciences, in particular food sciences/technology to CB and JT]. We also benefited from funding from the French government, through the UCAJEDI "Investments in the Future" project managed by the ANR grant No. ANR-15-IDEX-01 (to SF and JG). Computation for the work described in this paper was supported by the Université Côte d'Azur's Center for High-Performance Computing.

Keywords: receptor • membrane protein • mutagenesis • bitter • GPCR

[1] B. Lindemann, Nature 2001, 413, 219-225.

[2] W. Meyerhof, in Reviews of physiology, biochemistry and pharmacology, Springer, 2005, pp. 37-72.

[3] K. L. Mueller, M. A. Hoon, I. Erlenbach, J. Chandrashekar, C. S. Zuker, N. J. Ryba, Nature 2005, 434, 225-229.

[4] aS.-J. Lee, I. Depoortere, H. Hatt, Nature Reviews Drug Discovery 2019, 18, 116-138; bS. Foster, K. Blank, L. See Hoe, M. Behrens, W. Meyerhof, J. Peart, W. Thomas, The FASEB Journal 2014, 28, LB572; cA. Malki, J. Fiedler, K. Fricke, I. Ballweg, M. W. Pfaffl, D. Krautwurst, Journal of leukocyte biology 2015, 97, 533-545.

[5] E. Adler, M. A. Hoon, K. L. Mueller, J. Chandrashekar, N. J. Ryba, C. S. Zuker, Cell 2000, 100, 693-702.

[6] X. Deupi, J. Standfuss, Current opinion in structural biology 2011, 21, 541-551.

[7] aQ. Zhou, D. Yang, M. Wu, Y. Guo, W. Guo, L. Zhong, X. Cai, A. Dai, W. Jang, E. I. Shakhnovich, eLife 2019, 8; bC. A. de March, Y. Yu, M. J. Ni, K. A. Adipietro, H. Matsunami, M. Ma, J. Golebiowski, Journal of the American Chemical Society 2015, 137, 8611-8616; cA.-M. Schönegge, J. Gallion, L.-P. Picard, A. D. Wilkins, C. Le Gouill, M. Audet, W. Stallaert, M. J. Lohse, M. Kimmel, O. Lichtarge, Nature communications 2017, 8, 1-12; dC. A. de March, J. Topin, E. Bruguera, G. Novikov, K. Ikegami, H. Matsunami, J. Golebiowski, Angewandte Chemie 2018, 130, 4644-4648.

[8] A. Di Pizio, A. Levit, M. Slutzki, M. Behrens, R. Karaman, M. Y. Niv, in Methods in cell biology, Vol. 132, Elsevier, 2016, pp. 401-427.

[9] aT. Sakurai, T. Misaka, M. Ishiguro, K. Masuda, T. Sugawara, K. Ito, T. Kobayashi, S. Matsuo, Y. Ishimaru, T. Asakura, Journal of Biological Chemistry 2010, 285, 28373-28378; bA. Brockhoff, M. Behrens, M. Y. Niv, W. Meyerhof, Proceedings of the National Academy of Sciences 2010, 107, 11110-11115; cN. Singh, S. P. Pydi, J. Upadhyaya, P. Chelikani, Journal of Biological Chemistry 2011, 286, 36032-36041; dR. Karaman, S. Nowak, A. Di Pizio, H. Kitaneh, A. Abu-Jaish, W. Meyerhof, M. Y. Niv, M. Behrens, Chemical biology & drug design 2016, 88, 66-75; eF. Fierro, A. Giorgetti, P. Carloni, W. Meyerhof, M. Alfonso-Prieto, Scientific reports 2019, 9, 1-16; fM. Sandal, M. Behrens, A. Brockhoff, F. Musiani, A. Giorgetti, P. Carloni, W. Meyerhof, Journal of chemical theory and computation 2015, 11, 4439-4449; gA. Di Pizio, L.-M. Kruetzfeldt, S. Cheled-Shoval, W. Meyerhof, M. Behrens, M. Y. Niv, Scientific reports 2017, 7, 1-11; hA. Thomas, C. Sulli, E. Davidson, E. Berdougo, M. Phillips, B. A. Puffer, C. Paes, B. J. Doranz, J. B. Rucker, Sci Rep 2017, 7, 7753; iX. Biarnés, A. Marchiori, A. Giorgetti, C. Lanzara, P. Gasparini, P. Carloni, S. Born, A. Brockhoff, M. Behrens, W. Meyerhof, PloS one 2010, 5; jS. Prasad Pydi, J. Upadhyaya, N. Singh, R. Pal Bhullar, P. Chelikani, Current Protein and Peptide Science 2012, 13, 501-508; kJ. P. Slack, A. Brockhoff, C. Batram, S. Menzel, C. Sonnabend, S. Born, M. M. Galindo, S. Kohl, S. Thalmann, L. Ostopovici-Halip, Current Biology 2010, 20, 1104-1109; lY. Wang, A. L. Zajac, W. Lei, C. M. Christensen, R. F. Margolskee, C. Bouysset, J. Golebiowski, H. Zhao, S. Fiorucci, P. Jiang, Chemical senses 2019, 44, 339-347.

[10] C. A. de March, S. K. Kim, S. Antonczak, W. A. Goddard III, J. Golebiowski, Protein Science 2015, 24, 1543-1548.

[11] aL. Charlier, J. Topin, C. Ronin, S.-K. Kim, W. A. Goddard, R. Efremov, J. Golebiowski, Cellular and molecular life sciences 2012, 69, 4205-4213; bC. Bushdid, A. Claire, J. Topin, M. Do, H. Matsunami, J. Golebiowski, Cellular and molecular life sciences 2019, 76, 995-1004.

[12] J. A. Ballesteros, H. Weinstein, in Methods in neurosciences, Vol. 25, Elsevier, 1995, pp. 366-428.

[13] V. Katritch, G. Fenalti, E. E. Abola, B. L. Roth, V. Cherezov, R. C. Stevens, Trends in biochemical sciences 2014, 39, 233-244.

[14] Y. Miao, S. E. Nichols, P. M. Gasper, V. T. Metzger, J. A. McCammon, Proceedings of the National Academy of Sciences 2013, 110, 10982-10987.

[15] A. Venkatakrishnan, X. Deupi, G. Lebon, C. G. Tate, G. F. Schertler, M. M. Babu, Nature 2013, 494, 185-194.

[16] D. P. Staus, R. T. Strachan, A. Manglik, B. Pani, A. W. Kahsai, T. H. Kim, L. M. Wingler, S. Ahn, A. Chatterjee, A. Masoudi, Nature 2016, 535, 448-452.

[17] B. Wu, E. Y. Chien, C. D. Mol, G. Fenalti, W. Liu, V. Katritch, R. Abagyan, A. Brooun, P. Wells, F. C. Bi, Science 2010, 330, 1066-1071.

[18] S. Nowak, A. Di Pizio, A. Levit, M. Y. Niv, W. Meyerhof, M. Behrens, Biochimica et Biophysica Acta (BBA)-General Subjects 2018, 1862, 2162-2173.

[19] D. Kim, S. Cho, M. A. Castaño, R. A. Panettieri, J. A. Woo, S. B. Liggett, American journal of respiratory cell and molecular biology 2019, 60, 532-540.

[20] T. Flock, A. S. Hauser, N. Lund, D. E. Gloriam, S. Balaji, M. M. Babu, Nature 2017, 545, 317-322.

Entry for the Table of Contents

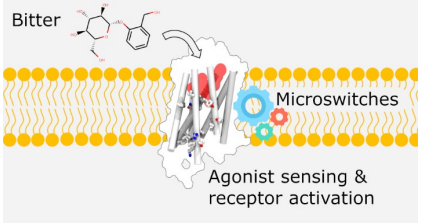

Bitter taste receptors are G protein-coupled receptors. We identified how receptors agonist sensing and downstream signaling is encoded into conserved sequence motifs.